The International Maritime Transport and Logistics (MARLOG 15) - ISSN 2974-3141
http://dx.doi.org/10.21622/MARLOG.2026.15.1.69
Smart & Resilient Logistics Corridors Future Gateway to the Green Trade

# Numerical Prediction of the Potential Tsunami Wave Heights and Inundation Zones for the Coastal Region of Alexandria, Egypt

**Mohamed M. Abouelnasr[1] and Akram S. Elselmy[2]**

*(1) Arab Academy for Science, Technology and Maritime Transport, Alexandria, Egypt; M.Abouelnasr5432@student.aast.edu*

*(2) Arab Academy for Science, Technology and Maritime Transport, Alexandria, Egypt; Akram_soliman@aast.edu*

***Keywords:*** Alexandria, ComMIT, Numerical Modelling, Mediterranean, Tsunami Simulation.

## ABSTRACT

The escalating susceptibility of Mediterranean coastal communities to tsunami threats necessitates the implementation of comprehensive, data-informed solutions that connect coastal modelling with effective risk reduction. This work utilizes high-resolution numerical simulations to assess the effects of tsunamis produced by various seismic return periods on Alexandria and Eastern Mediterranean Sea. The study employs a scenario-based methodology to quantify essential tsunami parameters, including wave height, flood extent, withdrawal amplitudes, and current velocities, for earthquake magnitudes between Mw 7.15 and Mw 8.5. The findings indicate a nonlinear increase in hazard intensity with rising magnitude, resulting in extreme situations where flood areas reach 114 $km^2$ and current speeds approach 20 m/s. These findings reveal possible shortcomings in current planning frameworks that emphasize moderate return periods while neglecting the catastrophic possibility of low-probability, high-impact occurrences. The study advocates for a paradigm shift in coastal infrastructure development, asserting that design standards and zoning rules must be adjusted to account for both probable situations and worst-case estimates. Moreover, it promotes the incorporation of early warning indicators, such as substantial sea withdrawals. The suggested techniques are not solely technical solutions but integral to a comprehensive vision for safeguarding Alexandria from severe coastal threats. This study advances a novel approach to coastal risk management that is proactive, inclusive, and grounded on scientific coastal principles.

## 1. INTRODUCTION

The development of coastal risk assessment and mitigation planning frameworks is rooted in empirical data and numerical studies of the historical tsunami impacts. The historical tsunami records including the 2004 Sumatra and 1755 Lisbon events serve as a critical validation data for numerical models and are helpful to inform the realistic scenario development [1], [2]. Goda et al. [3], as well as Goda and Song [4], demonstrate that probabilistic methods that use stochastic source models and Monte Carlo simulations allow a detailed quantification of the uncertainty in tsunami risk assessment. The result of

these methodologies is not only the hazard maps that are produced but also the evacuation planning and the infrastructure vulnerability assessments that are carried out accordingly by considering the local topography, population density, and building characteristics [5], [6]. The compilation of historical data and multidisciplinary approaches are necessary for the areas with fewer tsunami records, promoting the identification of possible sources and recurrence patterns [7]. Dilek et al. [8] demonstrate that practical risk reduction can only be achieved with the contribution of scientists, policymakers, and communities to change the findings of research into real-life applications, for example in the form of mitigation strategies and emergency preparedness plans.

Research into tsunami hazards in the Mediterranean has evolved alongside advances in numerical modelling capabilities, high-resolution geospatial datasets, and a more refined grasp of regional tectonic frameworks. Many coastal areas within this basin, such as Alexandria and southern Sicily, are exposed to a variety of potential tsunami sources. These can originate from seismic events linked to fault displacement, volcanic activity that generates atmospheric pressure waves capable of exciting long ocean waves, or submarine landslides whose dynamics can produce devastating run-up heights under certain conditions [9]-[28]. The complexity lies in the diversity of source mechanisms and their interaction with unique local bathymetric and topographic settings. This interplay shapes the propagation, refraction, and amplification patterns of tsunami waves before they reach the shore. Simulations allow researchers to capture wave morphologies over time and space, which can be essential for identifying sectors at heightened risk [13], [15], [17], [22], [27]-[56].

Although there are several studies that have studied the possible tsunami waves for Alexandria, Egypt, there is current gap for the numerical prediction of the potential tsunami wave heights and inundation zones for the coastal region for different return periods, such as 475-year, 2475-year, and 4975-year of 10 %, 2 %, and 1% exceedance percentage in 50-year return period, respectively [9]-[26], [32], [57]. This study predicts numerically the potential tsunami wave heights and inundation zones for the coastal region of Alexandria, Egypt, following a numerical methodology for defined return periods, as illustrated in Figure 1.

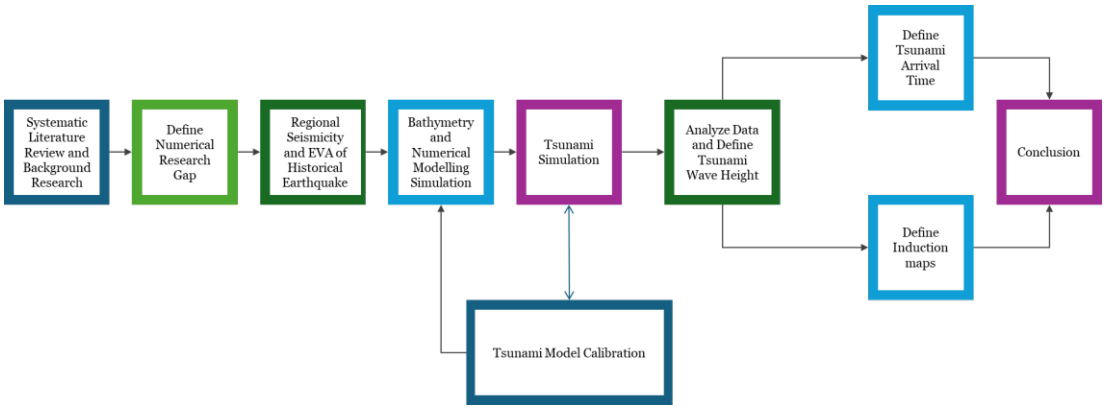


*Figure 1: Numerical Methodology Flow Chart followed for the Study*

Hypothetical earthquake scenarios have been used to estimate that nearly 85,000 people (15.8% of Alexandria's total population) are in tsunami hazard zones [20], while Pagnoni et al. [22] calculate that there are more than 12,000 buildings might be affected with 150,000 residents living in vulnerable districts.

## 2. SYSTEMATIC LITERATURE REVIEW

Tsunami waves and inundated areas are the visible effects of interrelated geophysical processes, starting from the source and propagating to the coastal impact. In their simplest state, tsunamis are long gravity waves that act like them, having wavelengths from tens of kilometres to hundreds of kilometres and periods from a few minutes to more than an hour [9], [27], [29], [36], [58], [59]. In deep water, tsunami waves have speeds approximated by Eq (1) [60], [61]:

$$C = \sqrt{g\,h} \tag{1}$$

*where: h is water depth, and g is the gravitational acceleration*

PRISMA (Preferred Reporting Items for Systematic reviews and Meta-Analyses) methodology is adapted for research synthesis in the marine environment, as demonstrated by previous studies [62]-[68]. Scopus dataset [69], [70] and MARLOG Conference dataset [71] have been selected to perform a schematic literature review. The criteria of the schematic literature review shall contain the define search terms in either the title, abstract or the keywords of the articles. Meanwhile, the exclusion criteria shall exclude the articles that have been published prior to 1990 to ensure that the latest research trend of the tsunami effect in Mediterranean Sea is well presented. Following the advanced search order of "TITLE-ABS-KEY (tsunami OR tsunamis) AND (Mediterranean OR Alexandria)) AND PUBYEAR>1989", 720 studies have matched the search criteria, and 42 studies have been investigated in detail.

Figure 2 represents the yearly number of scientific articles published on the topic of tsunamis in the Mediterranean Sea from 1990 to 2025 according to a systematic literature review conducted based on the PRISMA method. The data reveal a propagating publication activity that only began in the early 2000s, peaked in between the years 2016 and 2022 with records of exceeding 50 publications for the year. The trend line supports the notion of a strong association and emphasizes the nonlinear pattern of increase, with a peak followed by the slight reduction in the past years. This tendency indicates that the volume of research concerning Mediterranean tsunamis have markedly increased in the period of the last two decades mainly due to the growing environmental hazard awareness, progress in technology, and the inclusion of multiple disciplines, even though the recent decrease may indicate either maturing researches or the changes in academic priorities.

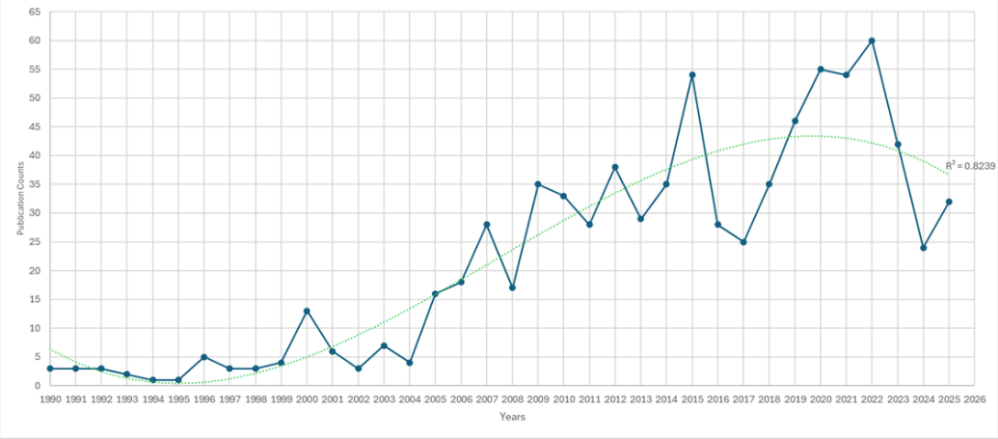


*Figure 2: The Quantities of Related Studies of Tsunami Waves for Alexandria, Egypt and/or Mediterranean Sea Region over the Last 35 Years*

Several articles predict the potential tsunami wave heights and inundation zones for the coastal region for different return periods [9]-[26], [32], [57]. Past tsunamis in the Mediterranean were proven with the combination of historical records and geological indicators found in coastal areas. Records linked with the seismic episodes were found on tectonic margins, the Hellenic Arc consists of West Hellenic Arc (WHA), East Hellenic Arc (EHA), and Cyprian Arc (CA), the shallow and large earthquakes, repeatedly nearby Hellenic Arc, were reported have been the reason for the destructive ocean wave generated that affected the large coastal areas [10]. Hamouda [72] and Stiros [25] define that the major tsunami events in 365 CE and 1303 CE had greatly affected parts of Egypt. Historically, offshore stratigraphic profiles can reveal mixed layers of tsunamis, coarse-grained sand deposits which are sharply emplaced above finer marine sediments [58]. Moreover, Eckert et al. [11] demonstrated that to determine inundation areas accurately it is necessary to link hydrodynamic modelling with detailed topographic mapping. One common strategy is to overlay maximum simulated computed water surface elevations on high-resolution digital elevation models (DEMs) that contain human elements like seawalls, embankment, or footprints of the buildings [1], [7], [13], [15], [17], [22], [27]-[32], [34]-[56].

In addition, Laksono et al. [27] demonstrate that the 2D digital elevation models (DEMs) are gathered into detailed bathymetric data to be distributed for hydrodynamics simulation purposes in composite grid formats. Nevertheless, Badreldin et al. [10] tried to integrate hazard assessment with exposure and evacuation analysis is on the rise. Tselentis et al. [50] and Rizzo et al. [73] demonstrate that there is a broad spectrum that goes from potential-driven evaluations which are based on the inclusion of several variables into a composite index to physics-based numerical solvers that solve nonlinear shallow water or Boussinesq equations for simulating long-wave phenomena. The utilization of advanced fluid dynamics codes is needed to have a precise comprehension of the small-scale processes or high bathymetric gradients. Nevertheless, these breakthroughs heavily depend on data quality; during the initial stages, the seabed mapping issues could be able to create big uncertainties on the flooded regions results.

Abouelnasr and Elselmy [74] demonstrate that the extreme coastal events can be numerically simulated via DHI MIKE21 FM SW and HD modules. Such investigations highlighted the concurrent dangers; storm surges can complicate tsunami action if both are present at the same time. Modelling of the extreme events support in forecasting of different scenarios later in the changed climate [74]-[76]. Moreover, lessons drawn from past events around the Mediterranean region show very important things for future assessments, such as the 2021 Algerian offshore earthquake caused tsunami that arrived in Southern France within 70-80 minutes [41]. Tselentis et al. [50] highlight that the lack of data makes it hard to create high-resolution maps for various sites that could potentially generate tsunamis; discrepancies in model selection come about, which causes the variance in predicted results; the interaction between different hazards, like tsunami generated by seismic events and meteorological surges, remains poorly quantified, even though the interest on it is increasing.

The conversion from seafloor deformation to surface displacement relies on vertical motion amplitude and spatial extent; uplift zones transfer positive anomalies to the free surface while subsidence introduces depressions. The two areas form the typical leading crest-trough pattern that can be found in most seismic tsunamis [77]. The seismic source mechanism is the one that has the most power in determining the form of waves initially. Normal and thrust faulting are some of the faulting geometries that usually generate broader vertical displacements than strike-slip ruptures of the same level because they have a greater vertical component of motion [27], [58]. Variations in rupture

directionality complicate the radiated energy field, as well; synchronous faults are most likely to generate waves propagating perpendicularly from the fault plane, while the asynchronous movements can increase the oblique components that may actually take the energy to different places [27], [44], [58].

The scenario-based risk modelling and vulnerability mapping based on the historical tsunami records and coastal geomorphological studies that inform directly Alexandria's tsunami preparedness and mitigation planning are provided as a data foundation [9]-[26], [32], [57]. The evidence base is extensive, covering tsunamis studies, historical studies, and various risk assessments. Salama et al. [23] are the ones that gave the main geomorphological evidence with the use of 5 trenches and 12 sediment cores, which they compare with the tsunami deposits from the three significant historical earthquakes (365 AD, 1303 AD, 1870 AD). Thus, their study contributes to the understanding of the recurrence of the event in the area. This historical basis made it possible for different kinds of quantitative risk assessments. Although there are several studies that have studied the possible tsunami waves for Alexandria, Egypt, there is current gap for the numerical prediction of the potential tsunami wave heights and inundation zones for the coastal region for different return periods [9]-[26], [32], [57]. Table 1 summarizes the main related previous studies that have discussed the related points of this study of numerical studies of tsunami generation in Mediterranean Sea and Alexandria, Egypt, Probabilistic Tsunami Hazard Assessment (PTHA), and tsunami flood and induction zones.

*Table 1. Boundaries for Historical Records of earthquakes*

| | *Numerical studies of Tsunami Generation in Mediterranean Sea* | *Numerical studies of Tsunami Generation for Alexandria, Egypt* | *PTHA for Mediterranean Sea* | *Tsunami Flood and Induction Zones* |
|---|---|---|---|---|
| Related Studies | [22], [27], [34]-[37], [41], [43], [46], [47], [49]-[51], [55] | [13], [15]-[19], [22], [25], [40], [78], [79] | [3], [80]-[83] | [4], [7], [10], [11], [13], [15], [16], [20], [21], [26], [35], [36], [49], [65], [78]-[80] |

## 3. METHODOLOGY AND NUMERICAL MODELLING

### 3.1 Regional Seismicity and Extreme Value Analysis of Historical Earthquake

Regional Seismicity define that there are 6194 earthquakes [84]-[87] have been recorded from 320 AD till 2025 with Mw of 3.5 or higher for the eastern southern part of Mediterranean Sea, as defined in Table 2 and Figure 3.

*Table 2. Boundaries for Historical Records of earthquakes*

| *Historical Records of earthquake* | *Grid Extend - Longitude Start Boundary (degree)* | *Grid Extend - Longitude End Boundary (degree)* | *Grid Extend - Latitude Start Boundary (degree)* | *Grid Extend - Latitude End Boundary (degree)* |
|---|---|---|---|---|
| Grid Boundaries | 20 | 35 | 30 | 36 |

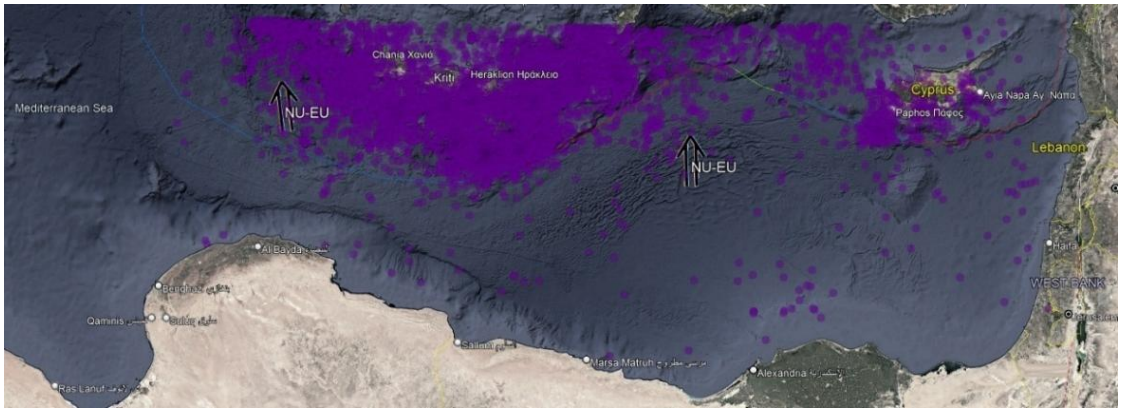


*Figure 3: Visualization of the Recorded 6194 Earthquakes Locations, from 320 AD till 2025 with Mw of 3.5 or Higher, for the Eastern Zone of Mediterranean Sea*

The defined dataset for extreme value analysis (EVA) are mainly gathered by United States Geological Survey (USGS) [84], [87] and European Archive of Historical Earthquake Data (AHEAD) [85], [86]. It is noticed that most of the earthquakes are located at the Hellenic Arc system [10], [88]. The Eastern Mediterranean is a highly seismically active region due to the complex interplay of the Anatolian, African, Arabian, and Eurasian plates. Faults are predominantly related to both strike-slip and thrust faulting, leading to both earthquakes and tsunamis [89]-[103]. It has major fault systems, such as the North Anatolian Fault Zone (NAFZ), East Anatolian Fault (EAF), Cyprus Arc, and Hellenic Subduction Zone [89]-[95]. Table 3 defines the earthquakes that have been recorded from 320 AD till 2025 with Mw of 7.3 or higher for the eastern part of Mediterranean Sea.

*Table 3. Historical Records of earthquakes from 320 AD till 2025 with Mw of 7.3 or higher for the eastern part of Mediterranean Sea [84], [87]*

| Year | Latitude (degree) | Longitude (degree) | Depth (km) | Magnitude (Mw) | Note |
|---|---|---|---|---|---|
| 365 | 35.06 | 24.94 | | 8.30 | Crete |
| 1222 | 34.70 | 32.60 | | 7.50 | Cyprus earthquake |
| 1903 | 35.40 | 23.30 | | 7.00 | Chania |
| 1903 | 35.72 | 25.80 | 8.0 | 8.26 | Crete |
| 1903 | 35.20 | 25.45 | 10.0 | 8.50 | Crete |
| 1904 | 35.50 | 23.30 | 1.0 | 7.50 | Crete |
| 1904 | 35.02 | 25.72 | 29.0 | 7.13 | Hierapetra |
| 1904 | 35.00 | 23.80 | 8.0 | 7.20 | Heraklio |
| 1904 | 35.00 | 23.70 | 9.0 | 7.30 | Crete |
| 1904 | 35.40 | 23.50 | 10.0 | 7.00 | Heraklio |
| 1904 | 35.90 | 22.90 | | 7.00 | Crete |
| 1904 | 35.50 | 25.60 | 16.0 | 7.50 | Heraklio |
| 1905 | 35.80 | 25.00 | 28.0 | 7.20 | Heraklio |
| 1905 | 35.60 | 25.80 | 12.0 | 7.70 | Heraklio |
| 1905 | 35.70 | 25.80 | 17.0 | 7.20 | Heraklio |
| 1905 | 36.00 | 23.00 | 80.0 | 7.90 | Southern Greece |
| 1905 | 35.64 | 27.16 | 15.0 | 7.30 | NNW of Karpathos, Greece |

The MIKE software suite, created by the Danish Hydraulic Institute (DHI) [76], [104]-[106], includes Extreme Value Analysis module (EVA), is used in this study for the extreme value analysis of the earthquakes. EVA has been conducted for the value noticed to gather the expected magnitude value of earthquake characteristics of 475-

year, 2475-year, and 4975-year of 10 %, 2 %, and 1% exceedance percentage in 50-year return period, respectively [75]. Log-Normal (Method of Moments) has been used for Extreme value Analysis [104], [105]. EVA results are accepted at a 0.06% level of significance. The hypothesis test is conducted by the module, and the null hypothesis was not rejected. Table 4 indicates the statistical and fit results for the EVA of the earthquakes. Badreldin et al. [10] defines the location of the extreme events, as shown in Figure 4. Figure 5 and Table 5 indicate expected magnitude value of earthquake characteristics of 475-year, 2475-year, and 4975-year of 10 %, 2 %, and 1% exceedance percentage in 50-year return period, respectively.

*Table 4. Historical Records of Earthquakes from 320 AD till 2025 with Mw of 7.3 or Higher for the Eastern Zone of Mediterranean Sea*

| Parameter | EVA Results |
|---|---|
| L-moments (L-1) | 3.780 |
| L-moments (L-2) | 0.36 |
| L-moments (Skewness) | 0.083 |
| L-moments (Kurtosis) | 0.145 |
| Log-Normal (Method of Moments) - Location parameter (fixed) | 1.00 |
| Log-Normal (Method of Moments) - Mean (log) | 0.994 |
| Log-Normal (Method of Moments) - Standard deviation (log) | 0.240 |
| Uncertainty calculation method | Monte Carlo method |


*Figure 4: Source Location of the Simulated Earthquake*

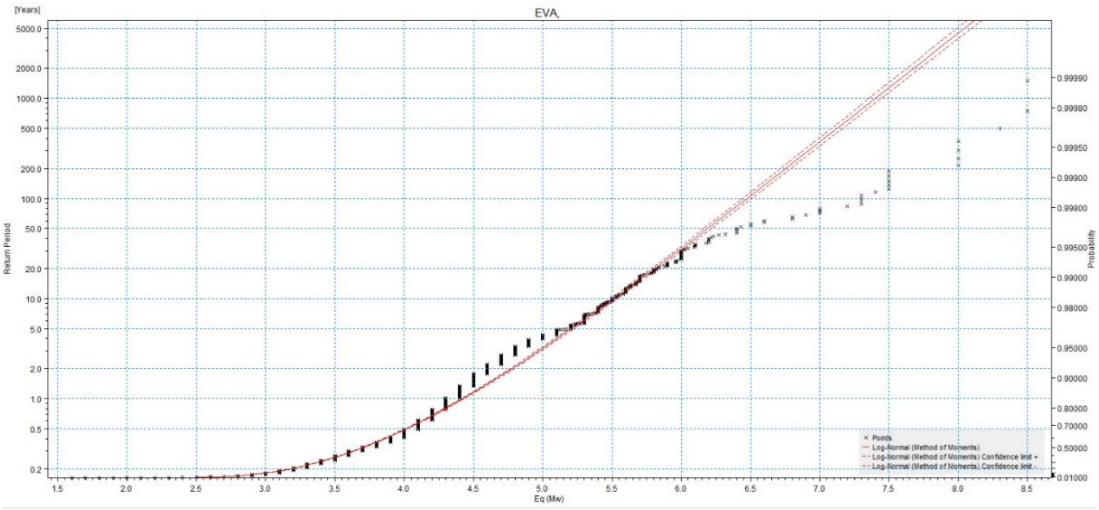


*Figure 5: Bathymetry and DEM data for different coverage zones (a) Grid A Bathymetry Extend, (b) Grid B Bathymetry Extend, (c) Grid C Bathymetry Extend, (d) Grid A, Grid B and Grid C coverage*

*Table 5. Historical Records of earthquakes from 320 AD till 2025 with Mw of 7.3 or higher for the eastern part of Mediterranean Sea*

| Year | 475-year (10 exceedance percentage in 50-year return period) | 2475-year (2 % exceedance percentage in 50-year return period) | 4975-year return period event (1% exceedance percentage in 50-year return period) | Extreme recorded estimated event [10], [18], [19], [25], [40] |
|---|---|---|---|---|
| Latitude (degree) | 35.01 | 35.01 | 35.01 | 35.01 |
| Longitude (degree) | 28.23 | 28.23 | 28.23 | 28.23 |
| Depth (km) | 10 | 10 | 10 | 10 |
| Magnitude (Mw) | 7.15 | 7.95 | 8.20 | 8.50 |
| Strike (degree) | 250 | 250 | 250 | 250 |
| Dip (degree) | 30 | 30 | 30 | 30 |
| Rake (degree) | 90 | 90 | 90 | 90 |
| Length (km) | 100 | 100 | 100 | 100 |
| Width (km) | 10 | 47 | 47 | 47 |
| Slip (m) | 2 | 5 | 14 | 39 |

## 3.2 Bathymetry and Shoreline Data

Bathymetry data [107]-[109], [31], [110] has been selected to cover 3 main grid areas with different, as defined in Table 6 and Figure 6.

*Table 6. Grid Extension of the Bathymetry and Numerical Modelling Simulation*

| GA with one-cut-point | Grid Extend - Longitude Start Boundary (degree) | Grid Extend - Longitude End Boundary (degree) | Grid Extend - Latitude Start Boundary (degree) | Grid Extend - Latitude End Boundary (degree) | Source [107]-[109], [31], [110] | Cell size (degree) | Total cells (degree) |
|---|---|---|---|---|---|---|---|
| Grid A | 20.000 | 36.500 | 30.000 | 40.000 | GEBCO and relevant datasets | 0.00 42 | 9504 000 |
| Grid B | 27.000 | 33.000 | 30.000 | 33.000 | GEBCO and relevant datasets | 0.00 42 | 1036 800 |
| Grid C | 28.800 | 30.200 | 30.750 | 31.750 | SRTM15 and relevant datasets | 0.00 42 | 8064 0 |

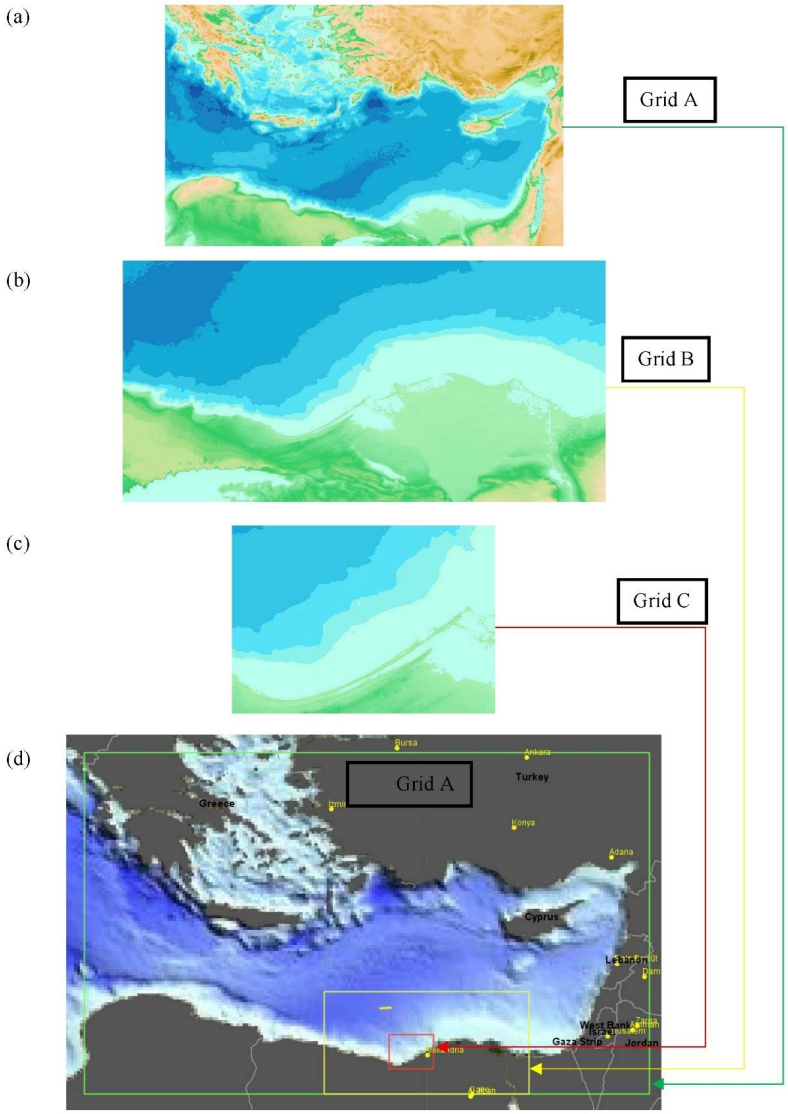


*Figure 6: Regional Bathymetry and DEM data for different coverage zones (a) Grid A Bathymetry Extend, (b) Grid B Bathymetry Extend, (c) Grid C Bathymetry Extend, (d) Grid A, Grid B and Grid C coverage*

### 3.3 Tsunami Simulation

The first step of Tsunami Simulation using ComMIT (Community Model Interface for Tsunami) [111], [112] is the initialization of the simulation environment and the definition of the earthquake source which is responsible for generating the tsunami. Table 5 is used to define the seismic scenarios or to define variables of the custom source such as fault location, depth, magnitude (Mw), the distribution of slip, rake, and rupture dimensions. The given parameters are converted then by the Okada model, which gives the vertical displacement of the seafloor due to fault motion, into an initial sea level surface deformation. The initial condition set for the future calculations of water wave surface propagation is determined as the initial sea level surface deformation.

ComMIT software has modeling limitations, such as the model dependence on nonlinear shallow water equations. Additionally, the accuracy of the model is dependent on either low-resolution grids or single Manning's roughness coefficients. The MOST ComMIT propagation model uses a numerical dispersion scheme and the non-linear shallow-water wave equations in spherical coordinates, as defined below in Eq (2) and Eq (3) [112], [113].

$$\frac{g\,D\gamma}{R\cos\varphi} + f\,v = u_t + \frac{u\,u\gamma}{R\cos\varphi} + \frac{v\,u\varphi}{R} + \frac{g\,h\gamma}{R\cos\varphi} \tag{2}$$

$$\frac{g\,D\varphi}{R} - f\,u = v_t + \frac{u\,v\gamma}{R\cos\varphi} + \frac{v\,v\varphi}{R} + \frac{g\,h\varphi}{R} \tag{3}$$

*Where: $\gamma$ is longitude, $\varphi$ is latitude, h is the amplitude, D is the undisturbed water depth, $u(\gamma,\varphi,t)$ is the depth-averaged velocity in longitude, $v(\gamma,\varphi,t)$ is the depth-averaged velocity in latitude directions. g is gravity acceleration. f is the Coriolis parameter. R is the Earth radius.*

The second step that follows the source definition is the propagation of tsunami through the deep ocean. The ComMIT using the MOST (Method of Splitting Tsunami) [111], [112], [114] model replaces the set of shallow water nonlinear equations with the nested grid as where the bottom is changing spatially. The third stage revolves around simulating coastal inundation through high-resolution nested grids and topographic data. Bathymetry data [107]-[109], [31], [110] has been selected to cover 3 main grid areas with different, as defined in Table 6 and Figure 7. Calibration run of 13th May 2025 Crete earthquake has been conducted [115], Sea level station monitoring gauge, located at 29.8853 ° Long, 31.2124 ° Lat is used for the model Calibration [116], as shown in Figure 7. Final step of tsunami simulation, defined in this study, presents the simulation of the 4 cases defined in Table 5 for a time span of 90 minute with a time step of 0.6 second for coastal zone of Alexandria, Egypt.

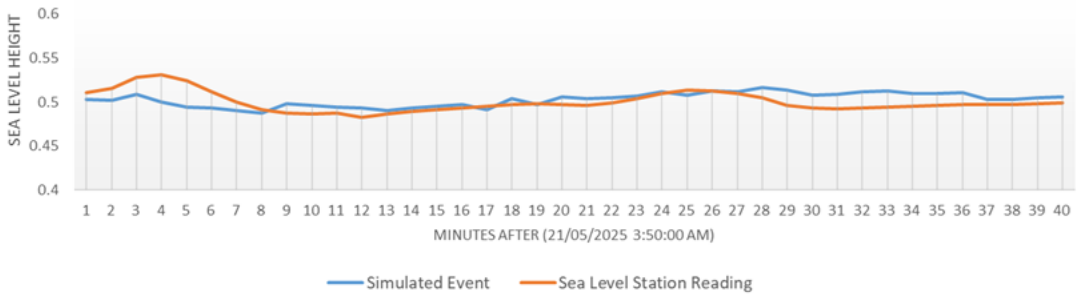


*Figure 7: Maximum Tsunami Wave Amplitude for Eastern Mediterranean Sea (a) Extreme recorded estimated event of Mw 8.5, (b) 4975-year*

## 4. RESULTS

Each of the four earthquake scenarios, defined in Table 5, is simulated by ComMIT and DHI MIKE HD [104], [105], [111], [112], [114]. The regional output includes the following data: tsunami travel time (arrival time), maximum amplitude (tsunami height), flow depth, and current speed.

Figure 8 presents the maximum tsunami amplitude, which refers to the peak height that seawater attains, and measured for the Eastern Mediterranean Sea with respect to Mean Sea Level (MSL) Datum. Observing the peak wave amplitude throughout the entire model run presents the maximum height for a given source at each position in the grid. During the entire run, the model captured maximum wave amplitudes at every grid point at 12-second intervals to create regional inundation maps.

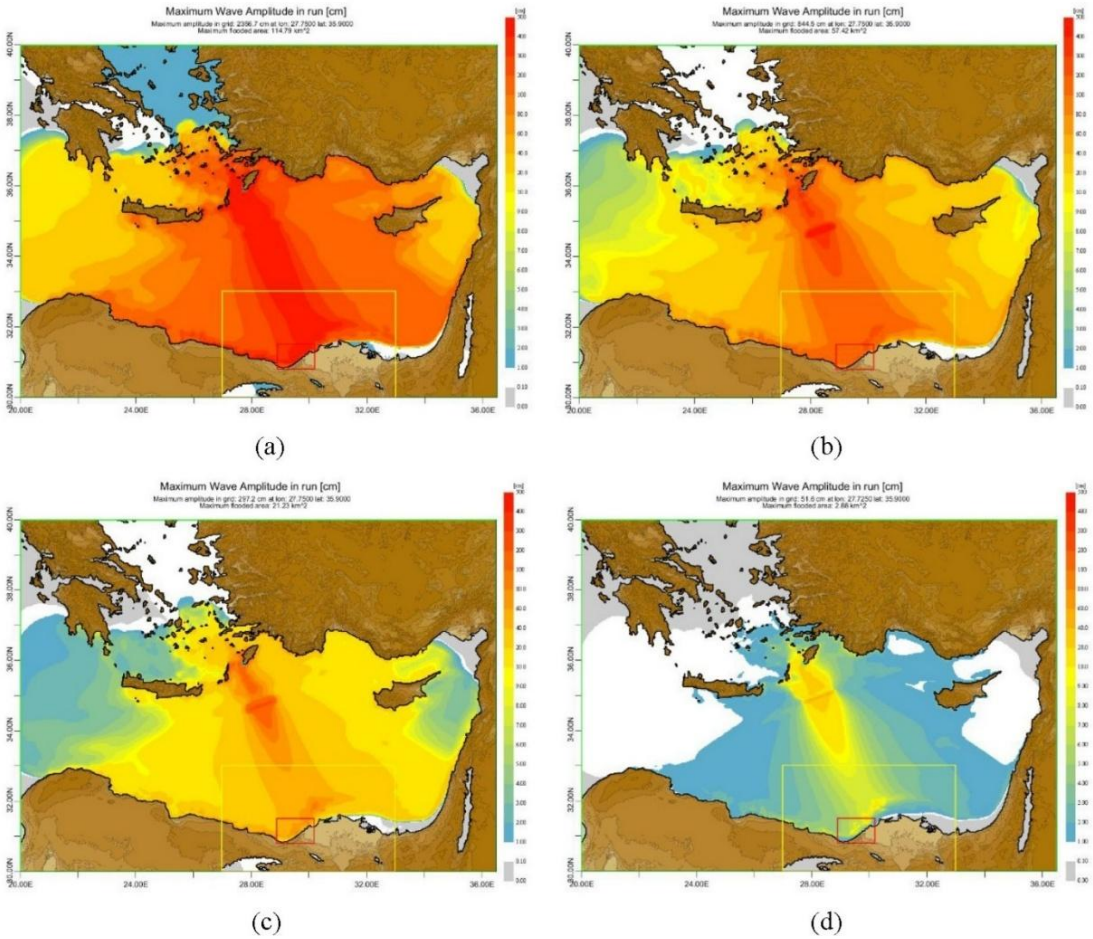


*Figure 8: Maximum Tsunami Wave Amplitude for Eastern Mediterranean Sea (a) Extreme recorded estimated event of Mw 8.5, (b) 4975-year return period event of Mw 8.2, (c) 2475-year return period event of Mw 7.95, (d) 475-year return period event of Mw 7.15*

On the nested level of Alexandria, Egypt, Figure 9 and Table 7 shows the maximum tsunami height that seawater attains and measured with respect to Mean Sea Level (MSL) Datum.

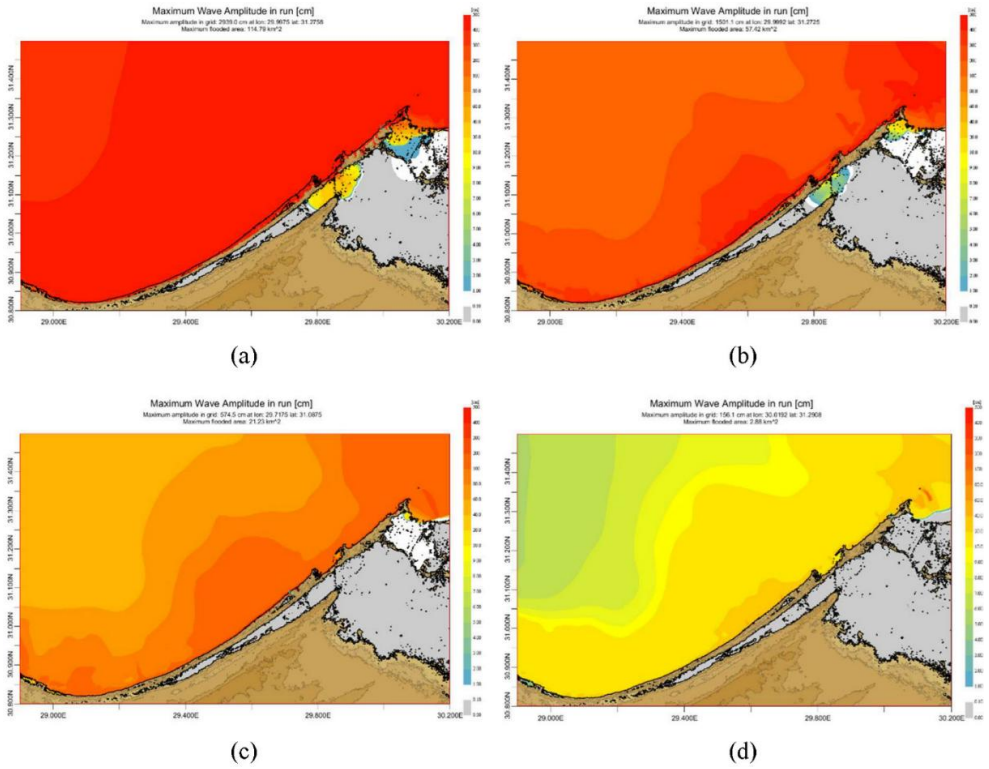


*Figure 9: Maximum Tsunami Wave Amplitude for Western Egypt (a) Extreme recorded estimated event of Mw 8.5, (b) 4975-year return period event of Mw 8.2, (c) 2475-year return period event of Mw 7.95, (d) 475-year return period event of Mw 7.15*

*Table 7. Maximum Tsunami Wave Amplitude and Flooded Area for Alexandria, Egypt*

| *Event Return Period* | *Maximum Tsunami Wave Amplitude (m)* | *Longitude Location of Maximum Tsunami Wave Amplitude (degree)* | *Latitude Location of Maximum Tsunami Wave Amplitude (degree)* | *Maximum Flooded Area (Km)* |
|---|---|---|---|---|
| 475-year event | 1.56 | 30.019 | 31.291 | 2.88 |
| 2475-year event | 5.75 | 29.718 | 31.088 | 21.23 |
| 4975-year event | 15.01 | 29.999 | 31.273 | 57.42 |
| Extreme recorded estimated event [10], [18], [19], [25], [40] | 29.39 | 29.996 | 31.276 | 114.79 |

Figure 10 and Figure 11 present the maximum withdrawal tsunami amplitude and measured with respect to MSL Datum for Eastern Mediterranean Sea and Alexandria, Egypt, respectively. Table 8 present the current speed due to tsunami amplitude for Alexandria, Egypt.

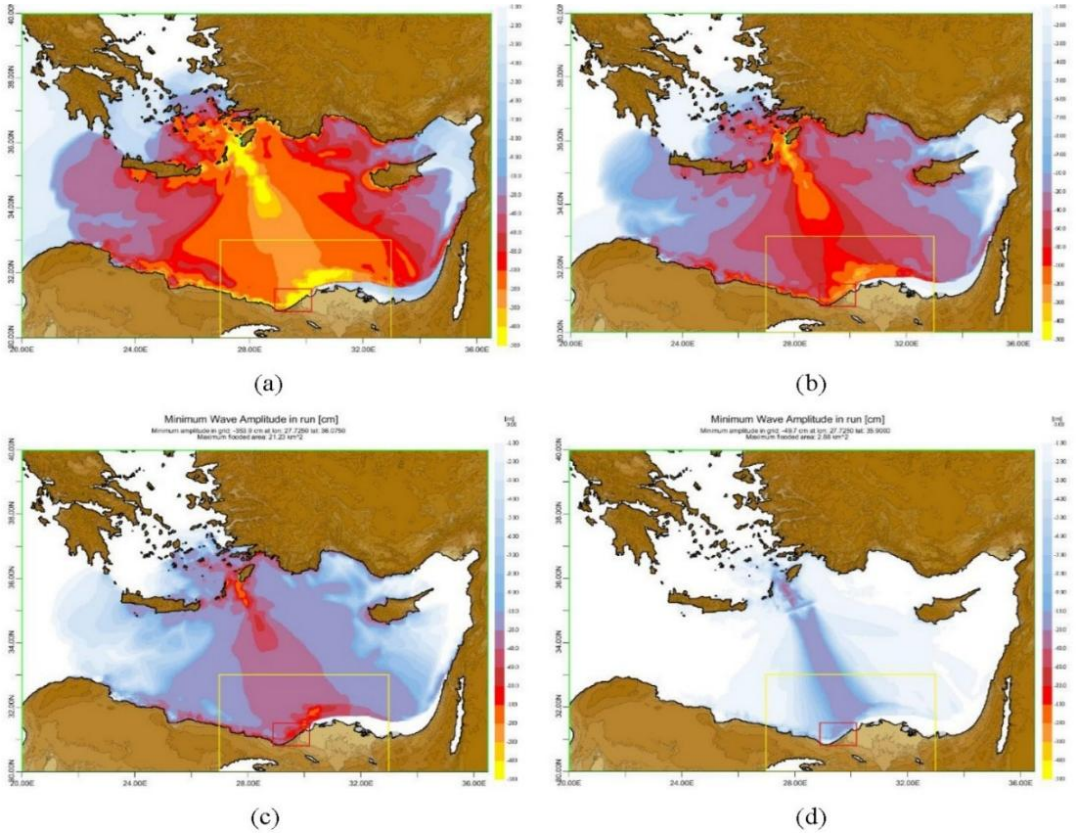


*Figure 10: Maximum Withdrawal Tsunami Wave Amplitude for Alexandria, Egypt (a) Extreme recorded estimated Event of Mw 8.5, (b) 4975-year return period event of Mw 8.2, (c) 2475-year return period event of Mw 7.95, (d) 475-year return period event of Mw 7.15*

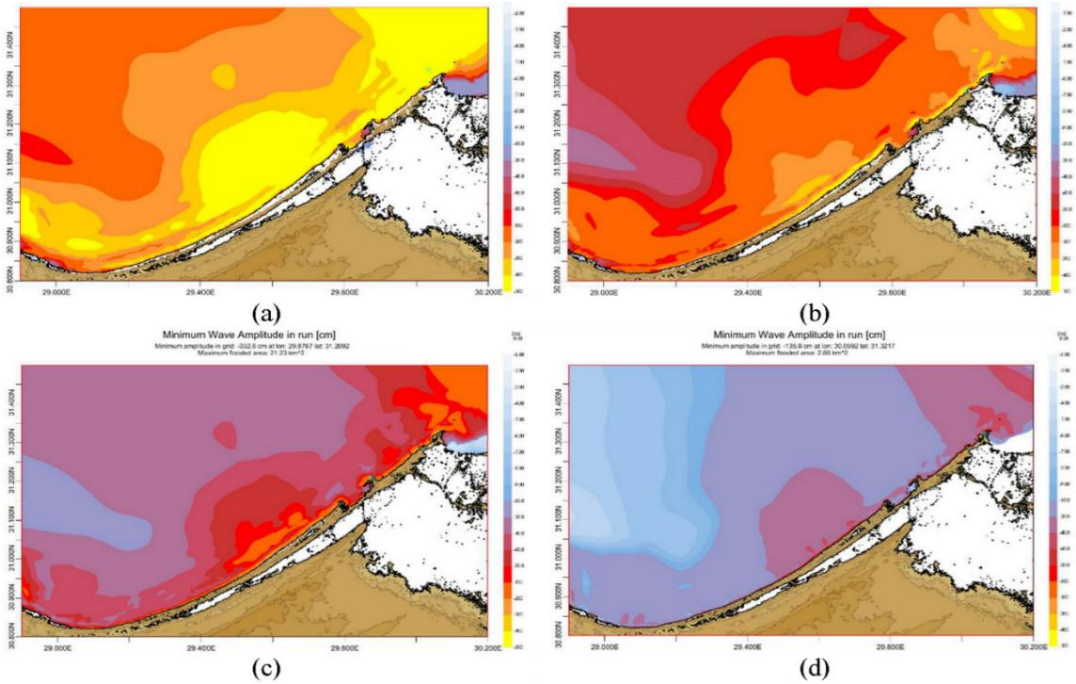


*Figure 11: Maximum Withdrawal Tsunami Wave Amplitude for Alexandria, Egypt (a) Extreme recorded estimated Event of Mw 8.5, (b) 4975-year return period event of Mw 8.2, (c) 2475-year return period event of Mw 7.95, (d) 475-year return period event of Mw 7.15*

*Table 8. Maximum Withdrawal Tsunami Wave Amplitude for Alexandria, Egypt*

| Event Return Period with Percentage of exceedance for 50-year design lifetime | Maximum Withdrawal Tsunami Wave Amplitude for Alexandria, Egypt | Longitude Location of Maximum Withdrawal Tsunami Wave Amplitude (degree) | Latitude Location of Maximum Withdrawal Tsunami Wave Amplitude (degree) |
|---|---|---|---|
| 475-year (10 exceedance percentage in 50-year design lifetime) | -1.36 | 30.059 | 31.322 |
| 2475-year (2 % exceedance percentage in 50-year design lifetime) | -3.33 | 29.877 | 31.209 |
| 4975-year return period event (1% exceedance percentage in 50-year design lifetime) | -6.52 | 30.003 | 31.287 |
| Extreme recorded estimated event [10], [18], [19], [25], [40] | -12.60 | 30.036 | 31.338 |

Figure 12 and Table 9 present the maximum current speed generated due to tsunami amplitude Alexandria, Egypt.

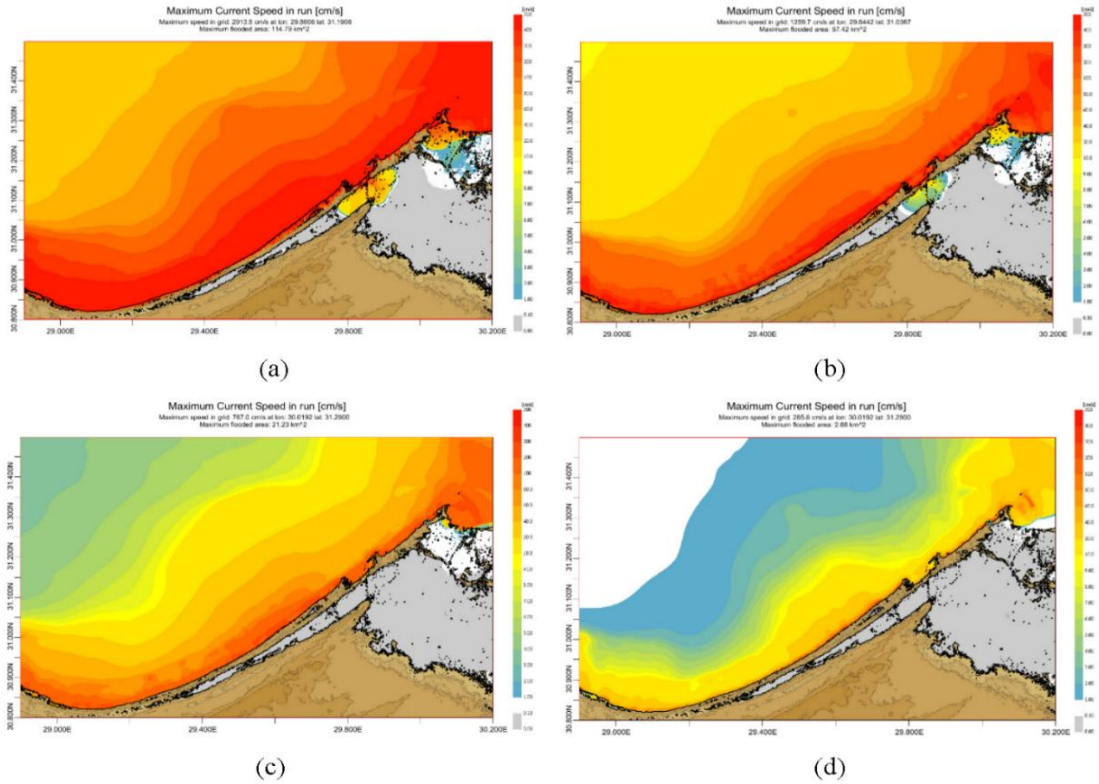


*Figure 12: Maximum Current Speed for Alexandria, Egypt (a) Extreme recorded estimated Event of Mw 8.5, (b) 4975-year return period event of Mw 8.2, (c) 2475-year return period event of Mw 7.95, (d) 475-year return period event of Mw 7.15*

*Table 9. Maximum Current Speed for Alexandria, Egypt*

| Event Return Period with Percentage of exceedance for 50-year design lifetime | Maximum Current Speed (m/s) | Longitude Location of Maximum Current due to Tsunami Wave (degree) | Latitude Location of Maximum Current due to Tsunami Wave (degree) |
|---|---|---|---|
| 475-year (10 exceedance percentage in 50-year design lifetime) | 2.86 | 30.019 | 31.290 |
| 2475-year (2 % exceedance percentage in 50-year design lifetime) | 7.67 | 30.019 | 31.290 |
| 4975-year return period event (1% exceedance percentage in 50-year design lifetime) | 12.60 | 29.644 | 31.037 |
| Extreme recorded estimated event [10], [18], [19], [25], [40] | 20.14 | 29.861 | 31.191 |

Figure 13 and Figure 14 illustrate time-series withdrawal tsunami wave amplitude for eastern side of Alexandria, located at 29.939° Long, 31.231° Lat, of the expected the water amplitude withdrawal of 4975-year return period event.

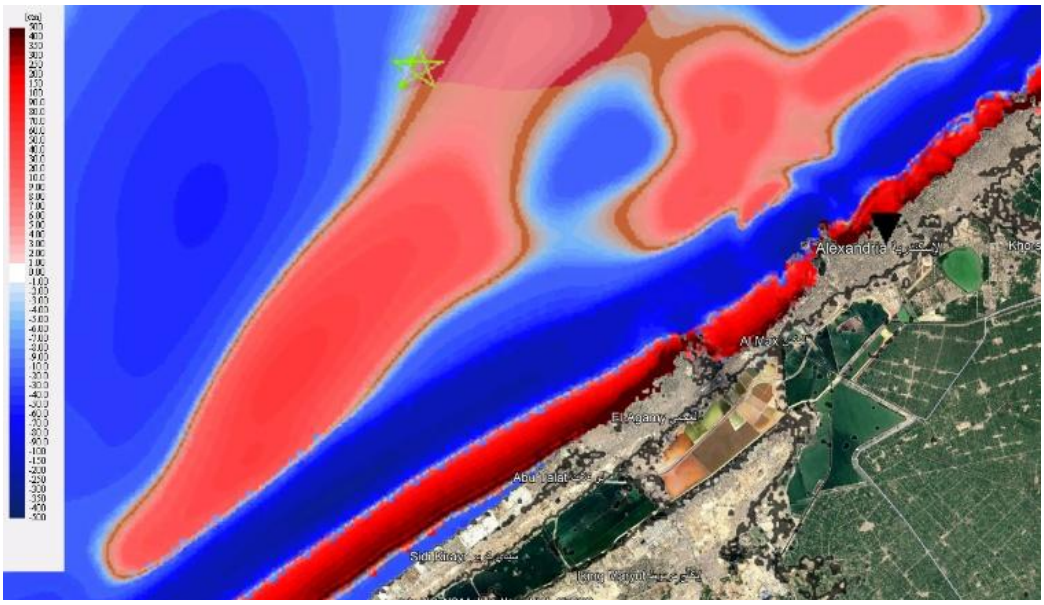


*Figure 13: Maximum Tsunami Wave Amplitude and Withdrawal Tsunami Wave Amplitude for Centre Alexandria of 4975-year return period event*

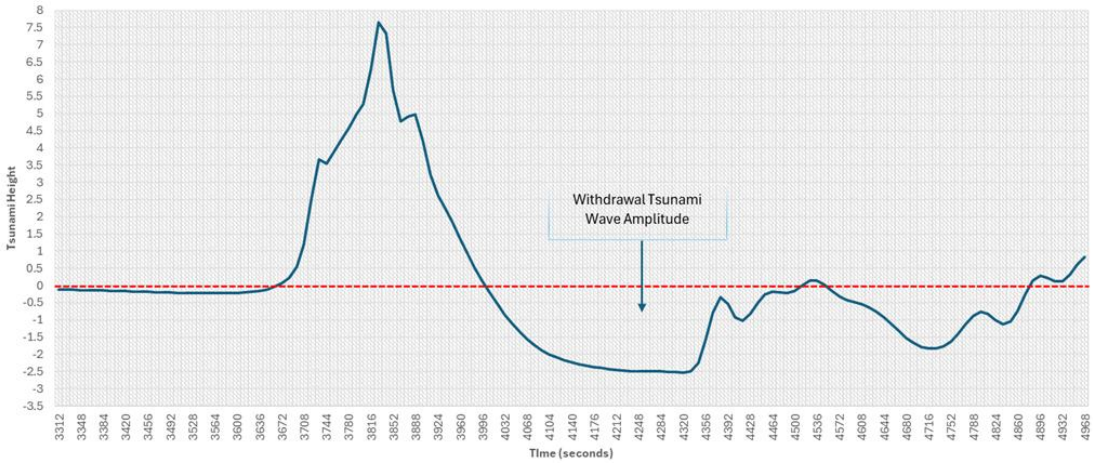


*Figure 14: Withdrawal Tsunami Wave Amplitude, located at 29.939° Long, 31.231° Lat Alexandria, for 4975-year return period event*

## 5. DISCUSSION

The notable methodological upgrades and data assimilation advancements in tsunamis as hazards in Alexandria have been progressivity elaborated in the recent decades. One of the compelling aspects of these improvements is the transition to high-resolution maps of individual seismic and tsunami hazards, which for the first time have been produced as a collaboration for an urban scale model [10]. High-resolution spatial details allow a more precise connection of the modelled hazard footprints to the actual urban morphology. The high-resolution outputs have direct application in intervention planning, coastal community sustainability, and multi-risk analyses [27]-[29], [36], [41], [45], [49]. Another advantage offered by some of the studies is the explicit pair-up of hazard modelling with assessments of vulnerability [11]-[13]. For instance, the identification of building fractions within the zones threatened by inundation under varied run-up scenarios can cede decision-makers with reliable metrics, including 42.93% for a 5 m run-up scenario and 48.95% for a 9 m scenario, linked to spatially explicit building-use data that highlight high-density residential exposure [13]. The mapping of tsunami risk zones that assimilate the previously mentioned hazard layers together with structural typologies is an example of the robust exchange of geophysical modelling and socio-economic impact evaluation [11], [12]. Another important advantage is the sustainable use of forward numerical simulations directed at potential seismic sources which are determined by regional seismotectonic no generic waveforms or transoceanic analogues [50].

Running various genetic mechanism scenarios has been a way of capturing certain source configurations, like the ones that create up to 4m waves at the key tourist resorts that should be monitored closely. These focused modelling techniques are in line with best practices in other Mediterranean sub-basins where source specificity has historically been the deciding factor in improving early warning parameters. Moreover, connecting the resilience assessment frameworks through modelled tsunamis not only reinforces the aspect of hazard mitigation beyond merely predicting flood extents; this strategic move allows understanding recovery potential under predetermined social and infrastructural conditions [13]. This results in matching technical modelling outcomes with the actual urban emergencies planning realities and adaptation requirements for the future. Things are double-sided, though, as there are persistent weaknesses that counterbalance the strengths. A typical hindrance is the lack of an integrated planning framework that directly connects scientific outputs to the legislative or urban development processes [24]. Despite creating detailed vulnerability and risk maps as well as locating areas of high

threat, several studies neglect to bind the conclusions within plan-in-force spatial planning indicators. This disconnection makes the use of advanced hazard analyses for proactive mitigation measures at the local municipal or governorate levels difficult. Besides, at times, the current attempts in hazard mapping have been of sectional nature; for example, as geophysical models are fine-tuned, institutional practices or coordination of preparedness strategies are still poorly developed in reference to the projected extent of future threats in Alexandria's coastal areas which are overcrowded. Uncertainty quantification is yet another domain where the literature is dissimilar and uneven. In this regard, some of the authors of the papers have mentioned explicitly that models such as simplified empirical equations are only real partially, hence their accuracy is highly dependent upon the quality and resolution of the input data [11], while others have only cursorily discussed the epistemic uncertainties linked to tsunami source characterization or recurrence intervals. The latest regional probabilistic tsunami hazard analysis (PTHA) instruments underline the gaps such as un-completed source catalogues, and unresolved scaling relationships between the magnitude of earthquakes and the height of the waves produced [82], [83], [117], [118].

In the Alexandria region, this might lead to the drawing of skewed hazard curves that could either overstate or understate the actual hazard due to the unrecorded incidences or the improperly characterized sources in the model priors. In the lack of sufficient calibration of the events, the previous studies result display many assumptions about local factors that remain with limited verification. In addition to this, the exposure assessments in some of the studies depend on building heights [27], [29], [45], [49]. Few Alexandria-specific studies have attempted joint scenario modelling. As a whole, the improvements in the spatial and socio-economic resolution, as well as in the specification of the sources, the exchange of social vulnerability among significant players are keys to Alexandria's tsunami hazard research [9]–[25].

The simulation work undertaken in this study is considered as a numerical assessment of the tsunami hazard for Alexandria, Egypt and the broader Eastern Mediterranean areas. The simulation results show that the ratio of different seismic return times to tsunami wave heights depends on the placing of earthquakes along the fault line. The data proves the data about the immense risk of the northern Egyptian coast being affected by significant flooding and deadly consequences due to rare, but major, offshore earthquakes. The constructive wave height, flooded area, and current speed with larger magnitude are significant coastal risks.

At the regional level, Figure 15 summarizes the positive relationship between tsunami wave amplitudes and earthquake magnitude. With a 475-year event (Mw 7.15), the wave height equals roughly 1.56 meters. A Mw 8.5 extreme event, it increases to a staggering 29.39 meters, which is 18 times the previous height, as noticed in Figure 13.

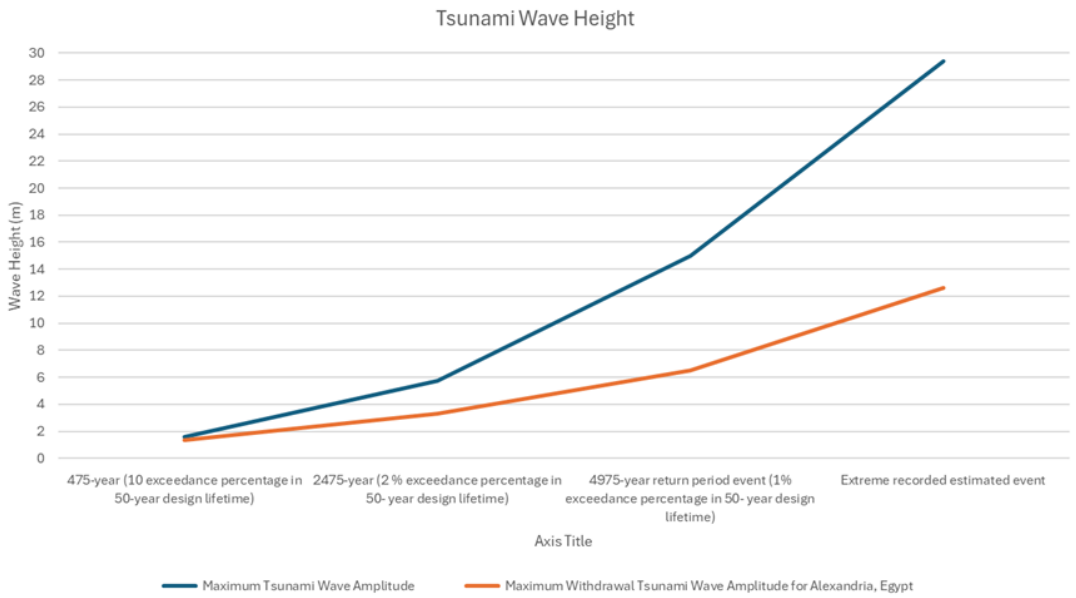


*Figure 15: Maximum Tsunami Wave Amplitude and Withdrawal Tsunami Wave Amplitude for Alexandria of different year return period of earthquake events*

Focusing on coastal zone of Alexandria, Table 7 and Figure 9 demonstrate that the flood area of Alexandria varies widely - from as low as 2.88 km$^2$ in the 475-year scenario to a whopping 114.79 km$^2$ in the worst-case Mw 8.5 simulation. The observed transformation of the situation from a local danger to a state of disaster gives one food for thought if the current preventive installations are adequate. A sizeable segment of the Alexandria population residing in the lowland areas may face colossal effects even from the moderate-return period scenarios. Thus, it will be essential to view the incorporation of tsunami hazard as a design-level issue, rather than a speculative risk alone.

The dynamic narrative is also powered by the captured withdrawal wave amplitudes that are expressed in Figures 10 to Figure 14. The waves that leave a withdrawal of water higher than -12.6 meters (indicating the early stage of water withdrawal) are hazardous and thus, act as a precursor for an impending tsunami. Noteworthy, it results in leaving exposed ground in dangerous areas, and thus, exposes themselves to be at risk of death, due to the super high-order wave drawdown.

In addition, the current speed profiles highlighted in Figure 12 and Table 9 once again bring out the underestimated magnitude of tsunami flows. For 475-year events, the current velocity can be as high as 2.86 m/s, which can endanger both human health and structural integrity. In fact, the figure surges to a dizzying 20.14 m/s in the extreme condition, which is enough to obliterate any port infrastructure, and disrupt exit routes. The simulated situations paint not one but two pictures, a potential tsunami and a future. The variation is dramatic depending on the magnitude and recurrence interval of the primary event. Vulnerability of infrastructure, critical assets and buildings should be studied to define the vulnerable risk identification for 475-year, 2475-year, and 4975-year of 10 %, 2 %, and 1% exceedance percentage in 50-year return period, respectively. In addition, as the duration of traveling for the first wave is 34 minutes for 4975-year return period event, it is recommended to use an early warning for tsunami for Alexandria, Egypt.

## 6. CONCLUSIONS

The progress made on tsunami hazards in the Mediterranean Sea, particularly in the Alexandria coastal area, is a result of the elaborated-progressive usage of high-resolution numerical modelling, geospatial datasets, and improved tectonic frameworks. Mainly, tsunami sources are considered a part to seismic fault displacement, volcanic forcing, and submarine landslides produce a troublesome environment for accurate hazard characterization.

Historical and geological evidence are necessary to interpret old tsunami events and to test models. These records are evidence for the Mediterranean tsunamis that have occurred sporadically over time yet with great intensity. The semi-enclosed basin shape of the Mediterranean, in addition to the varying coastline forms and bathymetric features, alters wave propagation, refraction, and amplification and thus differs from the open ocean tsunami. This yields to the fact that there will be different times for waves of other heights to reach the shore, which is a complication for early warning and evacuation planning. Theoretical perspectives that originate from the dynamics of shallow-water wave physics form a basis of the phylogenetic wave simulation itself, and the hydrodynamic simulations that accompany such waves display the processes involved in transferring waves from source to shore. The integration of socio-economic exposure data adds another layer to vulnerability assessments which is the identification of the critical infrastructure and the population that are at the highest risk during various temporal scenarios.

The study is informative about the possible hazards that Alexandria and Eastern Mediterranean coastal zone may face. The study applies sophisticated numerical models to the research for the examination of tsunami effects during various seismic return periods and magnitudes from moderate (Mw 7.15) to extreme (Mw 8.2 and Mw 8.5) cases. The outcomes indicate an incremental growth of hazard intensity with the progress of earthquake magnitude. Initially, the height of the tsunami waves was only a little over 1.5 meters but with the rise of the magnitude to the highest point, it jumped to almost 30 meters. At the outset, Alexandria's footprint maybe deteriorated under tsunami events as the flooded area expanded from 2.88 $km^2$ to over 114 $km^2$. The negative amplitudes in the withdrawal wave, often the initial indicators of a tsunami's approach, attain a magnitude of -12.6 meters, while flow velocities escalate to 20.14 m/s in the most extreme instances, posing a significant hazard to life and coastal infrastructure.

The results bring to fore the gap between the current preparedness levels and the expected potential of the hazards. The study urges a change to policy: disaster risk management should not just centre on probabilities but also on consequences and vulnerability. Zoning according to the scenarios, spatial development aligned with the extreme flow rates, and a broader public awareness campaign on early tsunami signals are some of the actions that should be performed without delay. It is recommended to develop a real-time forecasting system, which can do fast source invert and disseminate hazard, are all important directions for the way forward. The integration of detailed physical modelling with socio-economic matters focused on governance will be the path where the vulnerable centres of Alexandria shall be well protected against tsunamis in the future. Specific tsunami impact to Alexandria's port operations and associated nearshore and offshore infrastructures are recommended for future search.

## DECLARATION OF GENERATIVE AI AND AI-ASSISTED TECHNOLOGIES

During the preparation of this work, the author(s) used Scopus AI in order to define the main related articles that cover the topic as a part of the systematic literature search conducted. After using this tool/service, the authors reviewed and edited the content as necessary and took full responsibility for the content of the publication.

## 7. REFERENCES

[1] M. V. R. Murthy, T. Usha, Y. Pari, and N. T. Reddy, "Tsunami Vulnerability Assessment of Cuddalore Using Numerical Model and GIS," Marine Geodesy, vol. 34, no. 1, pp. 16-28, Feb. 2011.

[2] M. A. Ferreira, C. S. Oliveira, and R. Francisco, "Tsunami risk mitigation: the role of evacuation routes, preparedness and urban planning," Nat Hazards, vol. 121, no. 6, pp. 6719-6751, Apr. 2025.

[3] K. Goda, S. Li, N. Mori, and T. Yasuda, "Probabilistic Tsunami Damage Assessment Considering Stochastic Source Models: Application to the 2011 Tohoku Earthquake," Coastal Engineering Journal, vol. 57, no. 3, pp. 1550015-1-1550015-38, Sept. 2015.

[4] K. Goda and J. Song, "Uncertainty modeling and visualization for tsunami hazard and risk mapping: a case study for the 2011 Tohoku earthquake," Stoch Environ Res Risk Assess, vol. 30, no. 8, pp. 2271-2285, Dec. 2016.

[5] P. González-Riancho, I. Aguirre-Ayerbe, I. Aniel-Quiroga, S. Abad, M. González, J. Larreynaga, F. Gavidia, O. Q. Gutiérrez, J. A. Álvarez-Gómez, and R. Medina, "Tsunami evacuation modelling as a tool for risk reduction: application to the coastal area of El Salvador," Nat. Hazards Earth Syst. Sci., vol. 13, no. 12, pp. 3249-3270, Dec. 2013.

[6] J. H. Williams, T. M. Wilson, L. Wotherspoon, R. Paulik, E. M. Lane, N. Horspool, A. Weir, M. W. Hughes, M. R. Schoenfeld, D. Brannigan, A. Chalmers, and P. Elliot, "Tsunami damage and post-event disruption assessment of road and electricity infrastructure: A collaborative multi- agency approach in Ōtautahi Christchurch, Aotearoa New Zealand," International Journal of Disaster Risk Reduction, vol. 72, p. 102841, Apr. 2022.

[7] L. Pashova, L. Dimitrova, E. Oynakov, and V. Galabov, "Tsunami vulnerability along the western Bulgarian Black Sea coast - from the historical review towards multidisciplinary assessment approach," 04-Mar-2021. .

[8] Y. Dilek, Y. Ogawa, and Y. Okubo, "Characterization of modern and historical seismic-tsunamic events and their global-societal impacts," SP, vol. 501, no. 1, pp. 1-22, Jan. 2021.

[9] M. M. E. Abou-Mahmoud, "Assessing coastal susceptibility to sea-level rise in Alexandria, Egypt," Egyptian Journal of Aquatic Research, vol. 47, no. 2, pp. 133-141, 2021.

[10] H. Badreldin, H. Hassan, F. Romanelli, M. El-Hadidy, and M. N. ElGabry, "Joint Multi-Scenario-Based Earthquake and Tsunami Hazard Assessment for Alexandria, Egypt," Applied Sciences (Switzerland), vol. 14, no. 24, 2024.

[11] S. Eckert, R. Jelínek, G. Zeug, and E. Krausmann, "Remote sensing-based assessment of tsunami vulnerability and risk in Alexandria, Egypt," Applied Geography, vol. 32, no. 2, pp. 714-723, 2012.

[12] S. Eckert and G. Zeug, "Assessing Tsunami vulnerability in Alexandria, Egypt by using optical VHR satellite data," 2009, pp. 539-542.

[13] M. M. El-Hattab, S. A. Mohamed, and M. El-Raey, "Potential tsunami risk assessment to the city of Alexandria, Egypt," Environmental Monitoring and Assessment, vol. 190, no. 9, 2018.

[14] A. El-Sayed, F. Romanelli, and G. Panza, "Recent seismicity and realistic waveforms modeling to reduce the ambiguities about the 1303 seismic activity in Egypt," Tectonophysics, vol. 328, no. 3-4, pp. 341-357, 2000.
[15] S. Garziglia, M. Ioulalen, S. Migeon, E. Ducassou, J. Mascle, O. Sardou, and L. Brosolo, "Triggering factors and tsunamigenic potential of a large submarine mass failure on the western Nile margin (Rosetta Area, Egypt)," 2007, pp. 347-355.
[16] A. Hamouda, M. Hassan, and S. El-Gharabawy, "Enhancing tsunami resilience and evacuation strategies: A case study of coastal disaster preparedness and heritage protection of the Bibliotheca Alexandrina area," Egyptian Journal of Aquatic Research, vol. 50, no. 3, pp. 366-375, 2024.
[17] A. Z. Hamouda, "Numerical computations of 1303 tsunamigenic propagation towards Alexandria, Egyptian Coast," Journal of African Earth Sciences, vol. 44, no. 1, pp. 37-44, 2006.
[18] A. Z. Hamouda, "A reanalysis of the AD 365 tsunami impact along the Egyptian Mediterranean coast," Acta Geophysica, vol. 58, no. 4, pp. 687-704, 2010.
[19] A. Z. Hamouda, S. M. El-Gharabawy, A. Fekry, M. A. Nassar, and M. Salah, "Subsidence model of the ancient Alexandria Royal port linked to sea-level rise and natural hazards using integrated geophysical methods," Egyptian Journal of Aquatic Research, vol. 47, no. 3, pp. 283-292, 2021.
[20] H. M. Hassan, C. Frischknecht, M. N. ElGabry, H. Hussein, and M. ElWazir, "Tsunami hazard and risk assessment for Alexandria (Egypt) based on the maximum credible earthquake," Journal of African Earth Sciences, vol. 162, 2020.
[21] S. A. Mohamed, "Coastal vulnerability assessment using GIS-Based multicriteria analysis of Alexandria-northwestern Nile Delta, Egypt," Journal of African Earth Sciences, vol. 163, 2020.
[22] G. Pagnoni, A. Armigliato, and S. Tinti, "Scenario-based assessment of buildings' damage and population exposure due to earthquake-induced tsunamis for the town of Alexandria, Egypt," Natural Hazards and Earth System Sciences, vol. 15, no. 12, pp. 2669-2695, 2015.
[23] A. Salama, M. Meghraoui, M. ElGabry, S. Maouche, M. Hussein, and I. Korrat, "Paleotsunami deposits along the coast of Egypt correlate with historical earthquake records of eastern Mediterranean," Natural Hazards and Earth System Sciences, vol. 18, no. 8, pp. 2203-2219, 2018.
[24] M. A. Seddeek and M. M. Elsayed, "From Regional to Local Level: An Integrated Planning Framework for Cities Facing Tsunami Risk - Alexandria Case, Egypt," Civil Engineering and Architecture, vol. 10, no. 6, pp. 2230-2245, 2022.
[25] S. C. Stiros, "Was Alexandria (Egypt) destroyed in A.D. 365? A famous historical tsunami revisited," Seismological Research Letters, vol. 91, no. 5, pp. 2662-2673, 2020.
[26] M. Torab and N. Dalal, "Natural hazards mapping of mega sea waves on the northwest coast of Egypt," Elsevier Science Ltd., 2024, pp. 409-416.
[27] F. A. T. Laksono, M. Mishra, u. Fadlin, and J. Kovács, "Exploring the tsunami generation potential of major faults in the sicilian channel using 3D numerical modeling," Ocean Modelling, vol. 199, 2026.
[28] E. M. Bonilauri, C. Aaron, M. Cerminara, R. Paris, T. Esposti Ongaro, B. Calusi, D. Mangione, and A. J. L. Harris, "Inundation and evacuation of shoreline populations during landslide- Triggered tsunamis: An integrated numerical and statistical hazard assessment," Natural Hazards and Earth System Sciences, vol. 24, no. 11, pp. 3789-3813, 2024.
[29] A. Abbate, G. Davies, S. Lorito, N. Kalligeris, F. Romano, R. Tonini, and M. Volpe, "Importance sampling of seismic tsunami sources with near-field emphasis for

inundation PTHA: benchmarking with complete ensembles," Geophysical Journal International, vol. 241, no. 1, pp. 155-169, 2025.
[30] M. Abouelnasr, "Qualitative Numerical Statistical Analysis of the Extreme Wave Characteristics for Dubai Maritime City," p. 2551416 Bytes, 2020.
[31] M. Abouelnasr, "Extracted and Enhanced dataset of Mediterranean Sea Bathymetry for Numerical Modeling." Harvard Dataverse, 2022.
[32] M. Abouelnasr, "Dataset of prediction and mitigation process for coastal natural hazards for Alexandria, Egypt." [object Object], p. 3133096 Bytes, 2024.
[33] M. Abouelnasr, "Dataset of prediction and mitigation process for the coastal natural hazards for Alexandria, Egypt." Mendeley Data, 21-Feb-2024.
[34] L. Amir and A. Cisternas, "Appraisal of the 1790 Alboran tsunami source in the west Mediterranean sea as inferred from numerical modelling: Insights for the tsunami hazard in Algeria," 2010, vol. 6, pp. 4937-4945.
[35] S. Assier-Rzadkiewicz, P. Heinrich, P. C. Sabatier, B. Savoye, and J. F. Bourillet, "Numerical modelling of a landslide-generated tsunami: The 1979 nice event," Pure and Applied Geophysics, vol. 157, no. 10, pp. 1707-1727, 2000.
[36] L. Borzì, P. Scala, S. Distefano, F. X. A. T. Laksono, G. Manno, S. Innangi, F. Gamberi, J. Kovács, G. Ciraolo, and A. Di Stefano, "Tsunami propagation and flooding maps: An application for the Island of Lampedusa, Sicily Channel, Italy," Earth Surface Processes and Landforms, vol. 49, no. 14, pp. 4842-4861, 2024.
[37] M. Bubalo, I. Janeković, and M. Orlic, "Meteotsunami-related flooding and drying: numerical modeling of four Adriatic events," Natural Hazards, vol. 106, no. 2, pp. 1365-1382, 2021.
[38] C. Cecioni, G. Bellotti, P. De Girolamo, and L. FRANCO, "Full frequency dispersive numerical modelling of tsunamis. large scale application to the south tyrrhenian sea," presented at the Proceedings of the Coastal Engineering Conference, 2009, pp. 1337-1347.
[39] A. C. Demetracopoulos, C. Hadjitheodorou, and J. A. Antonopoulos, "Statistical and numerical analysis of tsunami wave heights in confined waters," Ocean Engineering, vol. 21, no. 7, pp. 629-643, 1994.
[40] A. Z. Hamouda, "Worst scenarios of tsunami effects along the Mediterranean coast of Egypt," Marine Geophysical Research, vol. 31, no. 3, pp. 197-214, 2010.
[41] P. Heinrich, A. Dupont, M. Menager, A. Trilla, A. Gailler, B. Delouis, and H. Hebert, "Simulation of the Mediterranean tsunami generated by the Mw 6.0 event offshore Bejaia (Algeria) on 18 March 2021," Geophysical Journal International, vol. 237, no. 3, pp. 1400-1413, 2024.
[42] A. Janin, M. Rodriguez, D. Sakellariou, V. Lykousis, and C. Gorini, "Tsunamigenic potential of a Holocene submarine landslide along the North Anatolian Fault (northern Aegean Sea, off Thasos island): Insights from numerical modelling," Natural Hazards and Earth System Sciences, vol. 19, no. 1, pp. 121-136, 2019.
[43] S. Le Roy, R. Pedreros, D. Monfort-Climent, and M. Terrier, "Numerical tsunamis simulations on the French Mediterranean coast: The case of Antibes," Houille Blanche, no. 6, pp. 12-20, 2015.
[44] M. Masina, R. Archetti, and A. Lamberti, "21 may 2003 boumerdès earthquake: Numerical investigations of the rupture mechanism effects on the induced tsunami and its impact in harbors," Journal of Marine Science and Engineering, vol. 8, no. 11, pp. 1-48, 2020.
[45] G. Paliaga, S. N. Ward, F. Luino, F. Francesco, and L. Turconi, "What If an Intense Rain Event Should Trigger Diffuse Shallow Landslides in a Small Mediterranean Catchment? Numerical Modeling Through Remote Sensing Techniques," Remote Sensing, vol. 16, no. 24, 2024.

[46] B. R. Röbke, H. Schüttrumpf, and A. Vött, "Effects of different boundary conditions and palaeotopographies on the onshore response of tsunamis in a numerical model - A case study from western Greece," Continental Shelf Research, vol. 124, pp. 182-199, 2016.
[47] B. R. Röbke, A. Vött, T. Willershäuser, P. Fischer, and H. Hadler, "Considering coastal palaeogeographical changes in a numerical tsunami model - A progressive base to compare simulation results with field traces from three coastal settings in western Greece," Zeitschrift fur Geomorphologie, vol. 59, pp. 157-188, 2015.
[48] J. Šepić, A. B. Rabinovich, and V. N. Sytov, "Odessa Tsunami of 27 June 2014: Observations and Numerical Modelling," Pure and Applied Geophysics, vol. 175, no. 4, pp. 1545-1572, 2018.
[49] E. Storrøsten, N. Ragu Ramalingam, S. Lorito, M. Volpe, C. Sánchez-Linares, F. Løvholt, and S. J. Gibbons, "Machine learning emulation of high resolution inundation maps," Geophysical Journal International, vol. 238, no. 1, pp. 382-399, 2024.
[50] G.-A. Tselentis, G. Stavrakakis, E. Sokos, F. Gkika, and A. Serpetsidaki, "Tsunami hazard assessment in the Ionian Sea due to potential tsunamogenic sources - Results from numerical simulations," Natural Hazards and Earth System Sciences, vol. 10, no. 5, pp. 1021-1030, 2010.
[51] M. Ulvrová, R. Paris, K. Kelfoun, and P. Nomikou, "Numerical simulations of tsunamis generated by underwater volcanic explosions at Karymskoye lake (Kamchatka, Russia) and Kolumbo volcano (Aegean Sea, Greece)," Natural Hazards and Earth System Sciences, vol. 14, no. 2, pp. 401-412, 2014.
[52] I. Vilibič, S. Monserrat, A. Rabinovich, and H. Mihanovič, "Numerical modelling of the destructive meteotsunami of 15 June, 2006 on the coast of the Balearic Islands," presented at the Pure and Applied Geophysics, 2008, vol. 165, no. 11-12, pp. 2169-2195.
[53] S. Yolsal-Cevikbilen and T. Taymaz, "Earthquake source parameters along the Hellenic subduction zone and numerical simulations of historical tsunamis in the Eastern Mediterranean," Tectonophysics, vol. 536-537, pp. 61-100, 2012.
[54] A. I. Zaitsev, A. Y. Babeyko, A. A. Kurkin, A. C. Yalçıner, and E. N. Pelinovsky, "Tsunami Hazard Assessment on the Egyptian Coast of the Mediterranean," Izvestiya, Atmospheric and Oceanic Physics, vol. 55, no. 5, pp. 462-469, 2019.
[55] F. Zaniboni, G. Pagnoni, G. Gallotti, M. Paparo, A. Armigliato, and S. Tinti, "Assessment of the 1783 Scilla landslide-tsunami's effects on the Calabrian and Sicilian coasts through numerical modeling," Natural Hazards and Earth System Sciences, vol. 19, no. 8, pp. 1585-1600, 2019.
[56] F. Zaniboni, G. Pagnoni, S. Tinti, M. Della Seta, P. Fredi, E. Marotta, and G. Orsi, "The potential failure of Monte Nuovo at Ischia Island (Southern Italy): Numerical assessment of a likely induced tsunami and its effects on a densely inhabited area," Bulletin of Volcanology, vol. 75, no. 11, pp. 1-13, 2013.
[57] M. Abouelnasr, "Raw Dataset for offshore Hindcast Waves data for 17 Ports along the Mediterranean Sea." Mendeley, 03-Jan-2023.
[58] F. X. A. T. Laksono, M. Mishra, B. Mulyana, and J. Kovács, "Exploring the Mediterranean tsunami research landscape: scientometric insights and future prospects," Geoenvironmental Disasters, vol. 11, no. 1, 2024.
[59] J. M. Abril and R. Periáñez, "A modelling study on tsunami propagation in the Red Sea: Historical events, potential hazards and spectral analysis," Ocean Engineering, vol. 134, pp. 1- 12, Apr. 2017.
[60] A. Joseph, Tsunamis: Detection, Monitoring, and Early-Warning Technologies. Elsevier, 2011.
[61] C. Finkl, "A Review of Potential Tsunami Impacts to the Suez Canal," Journal of Coastal Research, vol. 28, no. 4, p. 745, May 2012.

[62] M. S. Mohd Tahir, R. Mustapha, M. E. A. H. Hashim, N. Mohd Razalli, and A. Kleebrung, "Merging the Application of Artificial Intelligence Technology in Maritime Industry: A Systematic Literature Review," J. Adv. Res. Appl. Sci. Eng. Tech., pp. 19-34, Oct. 2024.

[63] C. Chlomoudis, A. Konstantinou, P. Kostagiolas, and P. Pallis, "Information needs and information-seeking behaviour of maritime students: a systematic literature review using the PRISMA method," LM, vol. 43, no. 5, pp. 353-369, Apr. 2022.

[64] F. Bojić, A. Gudelj, and R. Bošnjak, "Port-Related Shipping Gas Emissions-A Systematic Review of Research," Applied Sciences, vol. 12, no. 7, p. 3603, Apr. 2022.

[65] R. Abudu and R. Bridgelall, "Autonomous Ships: A Thematic Review," World, vol. 5, no. 2, pp. 276-292, Apr. 2024.

[66] G. Kodak, "Investigation of the Use of Multi-Criteria Decision-Making Techniques in Maritime Studies With Prisma Method," Marine Science and Technology Bulletin, vol. 12, no. 4, pp. 510- 521, Dec. 2023.

[67] A. Paraskevas, M. Madas, V. Zeimpekis, and K. Fouskas, "Smart Ports in Industry 4.0: A Systematic Literature Review," Logistics, vol. 8, no. 1, p. 28, Mar. 2024.

[68] M. J. Page, J. E. McKenzie, P. M. Bossuyt, I. Boutron, T. C. Hoffmann, C. D. Mulrow, L. Shamseer, J. M. Tetzlaff, E. A. Akl, S. E. Brennan, R. Chou, J. Glanville, J. M. Grimshaw, A. Hróbjartsson, M. M. Lalu, T. Li, E. W. Loder, E. Mayo-Wilson, S. McDonald, L. A. McGuinness, L. A. Stewart, J. Thomas, A. C. Tricco, V. A. Welch, P. Whiting, and D. Moher, "The PRISMA 2020 statement: an updated guideline for reporting systematic reviews," BMJ, p. n71, Mar. 2021.

[69] Elsevier, "ScienceDirect.com: Science, health and medical journals, full text articles and books.," 2025. [Online]. Available: https://www.sciencedirect.com/. [Accessed: 01-Sept-2025].

[70] Elsevier, "Scopus: A comprehensive abstract and citation database for impact makers," 2025. [Online]. Available: https://www.scopus.com. [Accessed: 01-Sept-2025].

[71] M. AASTMT, "The international Maritime Transport and Logistics Conference - AASTMT," The international Maritime Transport and Logistics Conference - AASTMT, 2025. [Online]. Available: https://marlog.aast.edu/en/home.

[72] A. Z. Hamouda, "A reanalysis of the AD 365 tsunami impact along the Egyptian Mediterranean coast," Acta Geophys., vol. 58, no. 4, pp. 687-704, Aug. 2010.

[73] A. Rizzo, G. Mattei, L. Dumon Steenssens, M. Anzidei, P. P. C. Aucelli, T. Alberti, F. Antonioli, A. Bezzi, D. Bonaldo, and G. Fontolan, "Methodological advances in sea level rise vulnerability assessment: implications for sustainable coastal management in a climate change scenario," Ocean and Coastal Management, vol. 268, 2025.

[74] M. Abouelnasr and A. Elselmy, "Medicanes and its Metrological Effects in the Mediterranean Sea: Case Study of Medicane Ianos," MARLOG 13 Conference, vol. 13, no. 1, p. 273, 2024.

[75] M. Abouelnasr, "Deformation and Stability Analysis of Double-Wall Vertical Breakwaters for Earthquake Return Periods," International Journal of Innovations in Engineering Research and Technology, vol. 7, no. 09, pp. 125-130, 2020.

[76] M. Abouelnasr, "Future Proof Infrastructure for Port-City: Case Study for the Sustainability of Suez Canal Entrance Groins Against Future Extreme Wave Conditions," MARLOG 12 Conference, vol. 1, no. 12, p. 174, Mar. 2023.

[77] A. El-Sayed, F. Romanelli, and G. Panza, "Recent seismicity and realistic waveforms modeling to reduce the ambiguities about the 1303 seismic activity in Egypt," Tectonophysics, vol. 328, no. 3-4, pp. 341-357, Dec. 2000.

[78] A. Fekry and A. Hamouda, "Hydrographic Surveys as an Art of Delineating the Impact of Climate Change on the Coastal Environment," MARLOG 11 Conference, vol. 11, no. 1, p. 99, 2022.
[79] A. Hamouda, "A re-analysis of the AD 365 tsunami impact along the Egyptian coast," 2007, vol. 1, pp. 269-282.
[80] M. B. Sørensen, M. Spada, A. Babeyko, S. Wiemer, and G. Grünthal, "Probabilistic tsunami hazard in the Mediterranean Sea," J. Geophys. Res., vol. 117, no. B1, p. 2010JB008169, Jan. 2012.
[81] S. J. Gibbons, S. Lorito, J. Macías, F. Løvholt, J. Selva, M. Volpe, C. Sánchez-Linares, A. Babeyko, B. Brizuela, A. Cirella, M. J. Castro, M. De La Asunción, P. Lanucara, S. Glimsdal, M. C. Lorenzino, M. Nazaria, L. Pizzimenti, F. Romano, A. Scala, R. Tonini, J. Manuel González Vida, and M. Vöge, "Probabilistic Tsunami Hazard Analysis: High Performance Computing for Massive Scale Inundation Simulations," Front. Earth Sci., vol. 8, p. 591549, Dec. 2020.
[82] I. Triantafyllou, G. A. Papadopoulos, and A. Kijko, "Probabilistic Tsunami Risk Assessment from Incomplete and Uncertain Historical Impact Records: Mediterranean and Connected Seas," Pure and Applied Geophysics, vol. 180, no. 5, pp. 1785-1809, 2023.
[83] A. Grezio, M. Anzidei, A. Armigliato, E. Baglione, A. Maramai, J. Selva, M. Taroni, A. Vecchio, and F. Zaniboni, "Tsunami hazard and risk in the Mediterranean Sea," Elsevier, 2024, pp. 397- 415.
[84] U.S. Geological Survey, "Lists, Maps, and Statistics - U.S. Geological Survey." [Online]. Available: https://www.usgs.gov/programs/earthquake-hazards/lists-maps-and-statistics. [Accessed: 01-Sept-2025].
[85] P. Albini, M. Locati, A. Rovida, and M. Stucchi, "European Archive of Historical EArthquake Data (AHEAD)." Istituto Nazionale di Geofisica e Vulcanologia (INGV), p. About 250 data sources, About 5000 earthquakes, About 3800 set of macroseismic intensity data points, About 70000 macroseismic intensity data points, 24-Jan-2013.
[86] G. A. Papadopoulos and A. Vassilopoulou, "Historical and Archaeological Evidence of Earthquakes and Tsunamis Felt in the Kythira Strait, Greece," in Tsunami Research at the End of a Critical Decade, vol. 18, G. T. Hebenstreit, Ed. Dordrecht: Springer Netherlands, 2001, pp. 119-138.
[87] D. M. Seal, A. Nowicki Jessee, and M. W. Hamburger, "Comprehensive Global Database of Earthquake-Induced Landslide Events and Their Impacts." U.S. Geological Survey, 2020.
[88] A. Ganas and T. Parsons, "Three-dimensional model of Hellenic Arc deformation and origin of the Cretan uplift," J. Geophys. Res., vol. 114, no. B6, p. 2008JB005599, June 2009.
[89] L. Gasperini, M. Stucchi, V. Cedro, M. Meghraoui, G. Ucarkus, and A. Polonia, "Active fault segments along the North Anatolian Fault system in the Sea of Marmara: implication for seismic hazard," Med. Geosc. Rev., vol. 3, no. 1, pp. 29-44, Mar. 2021.
[90] M. Palano, A. Ursino, S. Spampinato, F. Sparacino, A. Polonia, and L. Gasperini, "Crustal deformation, active tectonics and seismic potential in the Sicily Channel (Central Mediterranean), along the Nubia-Eurasia plate boundary," Sci Rep, vol. 10, no. 1, p. 21238, Dec. 2020.
[91] Y. D. Kuiper, A. Michard, E. Ruellan, C. S. Holm-Denoma, and J. L. Crowley, "New petrographic and U-Pb geochronology data from the Mazagan Escarpment, offshore Morocco: Support for an African origin," Journal of African Earth Sciences, vol. 181, p. 104249, Sept. 2021.
[92] X. Le Pichon, A. M. C. Şengör, J. Kende, C. İmren, P. Henry, C. Grall, and H. Karabulut, "Propagation of a strike-slip plate boundary within an extensional

environment: the westward propagation of the North Anatolian Fault," Can. J. Earth Sci., vol. 53, no. 11, pp. 1416-1439, Nov. 2016.

[93] M. Liu, X. Cui, and F. Liu, "Cenozoic rifting and volcanism in eastern China: a mantle dynamic link to the Indo-Asian collision?," Tectonophysics, vol. 393, no. 1-4, pp. 29-42, Nov. 2004.

[94] R. Lin, A. Vesnaver, G. Böhm, and J. M. Carcione, "Erratum for the paper: 'Broadband Q factor imaging by seismic tomography and instantaneous frequency,'" Geophysical Journal International, vol. 229, no. 2, pp. 898-899, Jan. 2022.

[95] S. Lorito, M. M. Tiberti, R. Basili, A. Piatanesi, and G. Valensise, "Earthquake-generated tsunamis in the Mediterranean Sea: Scenarios of potential threats to Southern Italy," J. Geophys. Res., vol. 113, no. B1, p. 2007JB004943, Jan. 2008.

[96] O. E. Frihy, K. M. Dewidar, and M. M. El Raey, "Evaluation of coastal problems at Alexandria, Egypt," Ocean & Coastal Management, vol. 30, no. 2-3, pp. 281-295, Jan. 1996.

[97] O. Frihy, S. Mohamed, D. Abdalla, and M. El-Hattab, "Assessment of natural coastal hazards at Alexandria/Nile Delta interface, Egypt," Environ Earth Sci, vol. 80, no. 1, p. 3, Jan. 2021.

[98] H. M. Hassan, C. Frischknecht, M. N. ElGabry, H. Hussein, and M. ElWazir, "Tsunami hazard and risk assessment for Alexandria (Egypt) based on the maximum credible earthquake," Journal of African Earth Sciences, vol. 162, p. 103735, Feb. 2020.

[99] Y. Z. Kamh, M. A. Khalifa, and A. N. El-Bahrawy, "Comparative Study of Community Resilience in Mega Coastal Cities Threatened by Sea Level Rise: The Case of Alexandria and Jakarta," Procedia - Social and Behavioral Sciences, vol. 216, pp. 503-517, Jan. 2016.

[100] G. Pagnoni, A. Armigliato, and S. Tinti, "Scenario-based assessment of buildings' damage and population exposure due to earthquake-induced tsunamis for the town of Alexandria, Egypt," Nat. Hazards Earth Syst. Sci., vol. 15, no. 12, pp. 2669-2695, Dec. 2015.

[101] S. C. Stiros, "Was Alexandria (Egypt) Destroyed in A.D. 365? A Famous Historical Tsunami Revisited," Seismological Research Letters, vol. 91, no. 5, pp. 2662-2673, Sept. 2020.

[102] B. L. Valle, N. Kalligeris, A. N. Findikakis, E. A. Okal, L. Melilla, and C. E. Synolakis, "Plausible megathrust tsunamis in the eastern Mediterranean Sea," Proceedings of the Institution of Civil Engineers - Engineering and Computational Mechanics, vol. 167, no. 3, pp. 99-105, Sept. 2014.

[103] G. Wöppelmann, G. Le Cozannet, M. De Michele, D. Raucoules, A. Cazenave, M. Garcin, S. Hanson, M. Marcos, and A. Santamaría-Gómez, "Is land subsidence increasing the exposure to sea level rise in Alexandria, Egypt?," Geophysical Research Letters, vol. 40, no. 12, pp. 2953- 2957, June 2013.

[104] DHI, "MIKE 21 Spectral Waves FM," DHI, The Netherlands, User Guide, 2017.

[105] DHI, "MIKE ZERO EVA," DHI, The Netherlands, User Guide MIKE ZERO Extreme Value Anaysis, 2019.

[106] M. Abouelnasr, "Qualitative Numerical Statistical Analysis of the Extreme Wave Characteristics for Dubai Maritime City," International Journal of Innovations in Engineering Research and Technology, vol. 7, no. 10, p. 2551416 Bytes, 2021.

[107] GEBCO Bathymetric Compilation Group 2025, "The GEBCO_2025 Grid - a continuous terrain model for oceans and land at 15 arc-second intervals." NERC EDS British Oceanographic Data Centre NOC, 2025.

[108] NSF OpenTopography Facility, "Global Bathymetry and Topography at 15 Arc Sec: SRTM15+V2.0." NSF OpenTopography Facility, 2019.

[109] B. Tozer, D. T. Sandwell, W. H. F. Smith, C. Olson, J. R. Beale, and P. Wessel, "Global Bathymetry and Topography at 15 Arc Sec: SRTM15+," Earth and Space Science, vol. 6, no. 10, pp. 1847-1864, Oct. 2019.

[110] M. Abouelnasr, "Extracted and Enhanced Dataset for Mediterranean Sea Shoreline." Harvard Dataverse, 2022.

[111] National Oceanic and Atmospheric Administration (NOAA), "ComMIT (COMmunity Model Interface for Tsunami)." [Online]. Available: https://nctr.pmel.noaa.gov/ComMIT/background.html. [Accessed: 01-Sept-2025].

[112] V. V. Titov, C. W. Moore, D. J. M. Greenslade, C. Pattiaratchi, R. Badal, C. E. Synolakis, and U. Kânoğlu, "A New Tool for Inundation Modeling: Community Modeling Interface for Tsunamis (ComMIT)," Pure Appl. Geophys., vol. 168, no. 11, pp. 2121-2131, Nov. 2011.

[113] Y. Okada, "Surface deformation due to shear and tensile faults in a half-space," Bulletin of the Seismological Society of America, vol. 75, no. 4, pp. 1135-1154, Aug. 1985.

[114] V. Titov, U. Kânoğlu, and C. Synolakis, "Development of MOST for Real-Time Tsunami Forecasting," J. Waterway, Port, Coastal, Ocean Eng., vol. 142, no. 6, p. 03116004, Nov. 2016.

[115] USGS National Earthquake Information Center, "USGS National Earthquake Information Center - M 6.0 - 20 km SSE of Fry, Greece," Earthquake Hazards Program, May-2025. [Online]. Available: https://earthquake.usgs.gov/earthquakes/eventpage/us7000pz2p/executive. [Accessed: 15-Oct-2025].

[116] National Institute of Oceanography and Fisheries, Alexandria, Egypt, University of Balearic Islands, Spain, and UNESCO Intergovernmental Oceanographic Commission (IOC), "Sea Level Station Monitoring Facility Database." Global Sea Level Observing System (GLOSS).

[117] A. Grezio, M. Anzidei, E. Baglione, B. Brizuela, P. Di Manna, J. Selva, M. Taroni, R. Tonini, and A. Vecchio, "Including sea-level rise and vertical land movements in probabilistic tsunami hazard assessment for the Mediterranean Sea," Scientific Reports, vol. 14, no. 1, 2024.

[118] G. A. Papadopoulos and I. Triantafyllou, "A Revision of Historical Earthquakes in the Ionian Sea, Greece: Island of Lefkada," GeoHazards, vol. 6, no. 1, 2025.